V. Communications Systems Research

ADVANCED ENGINEERING

A. Digital Acquisition and Detection: Digital Frequency Doubler, *G. Morris*

1. Introduction

In the design of digital systems, it is often necessary to have several different clock frequencies. It is quite easy to design digital frequency dividers with flip-flops. Here is given a presentation of a digital frequency doubler using only three integrated circuits and six discrete components (Fig. 1). This circuit has been evaluated in some experimental timing equipment in the DSIF frequency and timing subsystem at DSS 11. In this application, the doubler multiplied the available 5 MHz to 10 MHz to drive a counter. Previously, this doubling would have been done in an RF doubler which requires tuned circuits and would only operate at one frequency. The advantage of the digital doubler is that it can handle any frequency up to the maximum of the integrated circuits used, in this case, 20 MHz.

2. Theory of Operation

The active circuits are all Sylvania SUHL line integrated circuits. The SG-80 is a dual pulse shaper/delay *and* gate and the SG-340 is a quad two-input *nor* gate. The input signal is assumed to be a sine wave from a source which can deliver approximately 1 V rms into a 50-Ω load. This source is the DSIF standard. The SG-80 contains a regenerative Schmitt trigger which causes the output to snap to a logic "1" when the input signal rises to approximately 1.4 V. The output will snap to logic "0" when the input falls to approximately 0.8 V. This hysteresis gives a positive action which prevents multiple pulses when the input signal contains noise. The input coupling circuit of C1, C2, and R1 provides a 50-Ω load for the signal source. The potentiometer R2 is adjusted to obtain a square wave output from pin 12 of 1A.

The *nor* gate 2A is not absolutely necessary but is desirable so that 3A and 3B are both driven by identical circuits to obtain better symmetry and, hence, stability. The output from the Schmitt trigger is inverted by *nor* gate 2A for input to 3A. The output of 2A is inverted by 2B for input to 3A. Therefore, complimentary square wave signals are input to delay gates 3A and 3B. The delay circuits in 3A and 3B are controlled by the external capacitors C3 and C4. The delay is approximately 1.5 ns/pF. The 30-pF capacitors shown result in a delay of approximately 50 ns.

The frequency doubling is obtained by the delays in 3A and 3B. When 3A turns off, there is a delay determined by C4 before 3B turns on. During this interval, the output of *nor* gate 2C is high. When 3B turns off, there is a delay determined by C3 before 3A turns on. During this interval, the output of *nor* gate 2C is also high. Therefore, an output pulse is generated at both zero crossings of the input signal. The pulse widths of the output signal are

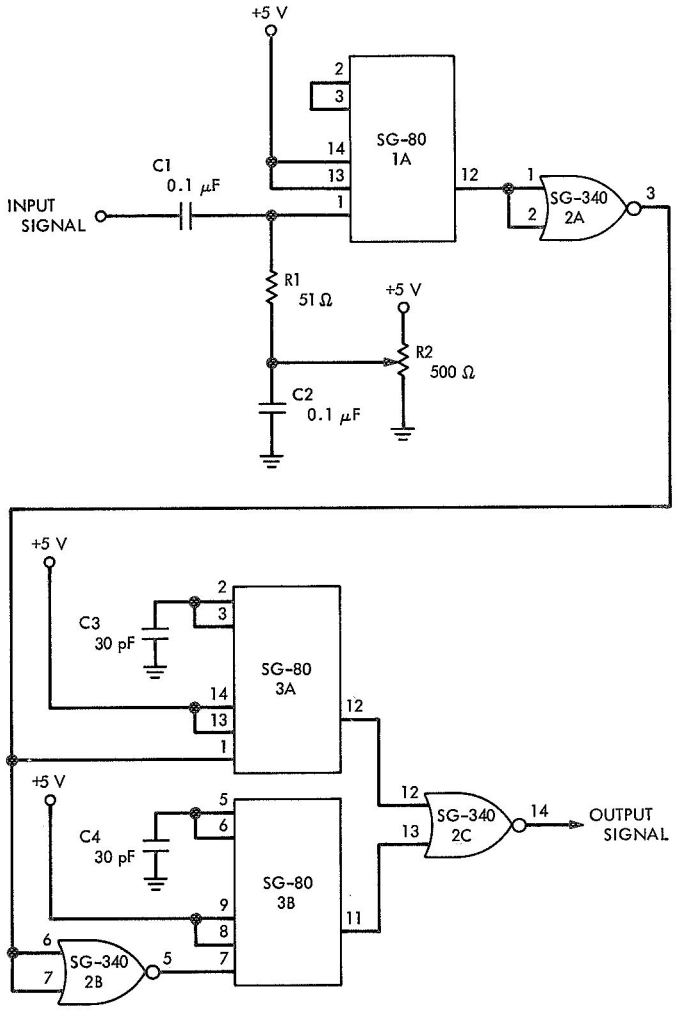

SG-80 DUAL PULSE SHAPER/DELAY AND GATE

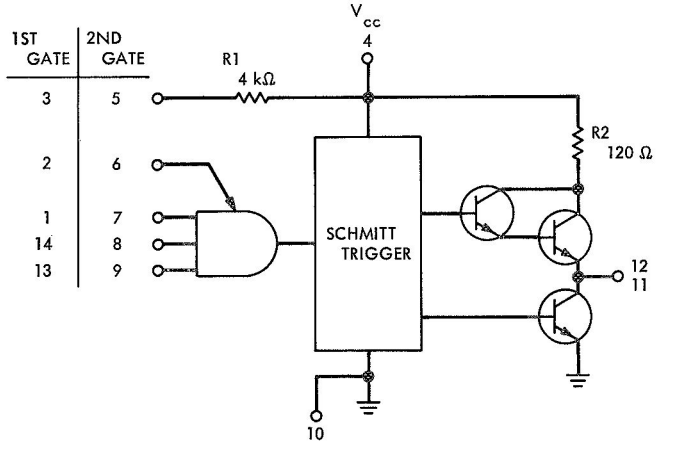

Fig. 1. Digital doubler schematic

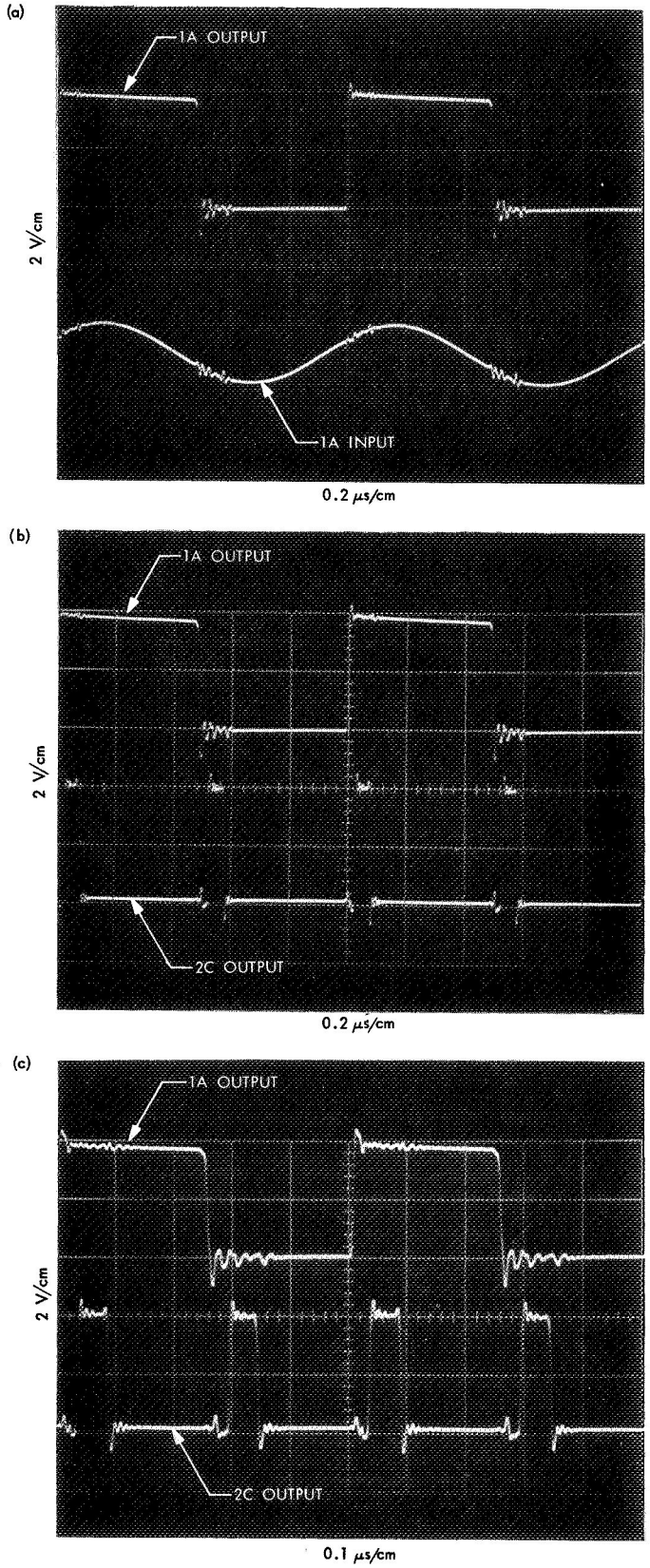

Fig. 2. Digital doubler oscilloscope waveforms

determined by capacitors C3 and C4 and are independent of the input frequency.

3. Experimental Results

Oscilloscope waveforms are shown in Fig. 2. The output of 1A is shown on the upper trace and the input to 1A is shown on the lower trace of Fig. 2a. The input signal is a 1-MHz sine wave. The output of 2C is shown on the lower trace of Fig. 2b. To demonstrate the fact that output signal pulse width is independent of frequency, the input signal is changed to 2 MHz in Fig. 2c. Note the sweep time is halved but the output pulse width remains constant.

B. Digital Telemetry and Command: A Collection of Results on Computational Complexity,

J. E. Savage[1]

1. Introduction

This article presents a variety of results obtained in our continuing effort to understand computational procedures and the effect of machine parameters on computation. The focus of this article is on a measure of "computational work" introduced earlier in the study of decoders for error correction.[2] We show that many different machines exist which compute simple and very complex functions with a computational work near the minimum required for these functions. We do not know whether the minimum can be approached when functions are neither very simple nor very complex. We consider computational procedures where the computation time depends on input data and the bound on the maximum time required for any data point. Bounds are also derived on the number of storage cells required to compute a function with an autonomous machine. In addition, we comment on the work potential of a computer which has many types of storage units attached to it and we offer a few remarks on the sorting problem. Finally, a simple quantum-mechanical bound is derived on the maximal complexity of functions which can be computed in t seconds with E ergs of energy.

All results are simply derived and follow from extensions of an inequality.[2] This inequality states that if the sequential machines $S_1, \cdots, S_k$ are interconnected to compute a function $f(\ )$, if they have the same cycle length and are constructed with logic elements from Ω and individually accessed memory cells, and if S_i has X_i logic elements and executes T_i cycles, then

$$\chi = \sum_{i=1}^{k} X_i T_i \geqq C_\Omega(f) \tag{1}$$

where $C_\Omega(f)$ is the minimum number of logic elements from Ω required to compute $f(\ )$ with a combinational machine. The quantity χ *is called computational work* and $C_\Omega(f)$ *is called the complexity of* $f(\ )$ *relative to* Ω. We note that the $C_\Omega(f)$ and $C_{\Omega'}(f)$ differ by at most a small constant factor since each element of Ω' can be replaced by a few elements from Ω and vice versa. For this reason, we let Ω be the set of 2-input binary logic elements and we assume that memory cells are binary.

2. A Bound on the Maximum Time to Compute a Function

The Inequality (1) assumes that for $1 \leqq i \leqq k$ the number of cycles for which S_i is used, namely, T_i, is fixed for the function $f(\ )$, that is, the T_i's do not depend on the arguments of the function. For many algorithms [which define finite functions $f(\ )$] the running time of the algorithm does depend on the data points. Consider, then, a single machine constructed with logic elements from Ω and individually accessed binary memory cells which computes $f(\ )$ with a variable number of cycles. Such a machine effectively has the power to turn off its own clock, since it stops at the end of its computation. If the machine is to be modified so that it always runs the same length of time on all data points [and so that Inequality (1) is applicable], the machine must be modified.

The value of the function must appear in the last state of the machine if its running time is variable. Thus, if the machine can be modified so that the value of the function

---

[1]Consultant, Division of Engineering, Brown University, Providence, R.I.

[2]Savage, J. E., "The Complexity of Decoders—Part II: Computational Work and Decoding Time," *IEEE Trans. Inform. Theory* (to be published).

computed can be saved and yet the machine is allowed to run until T_{max}, the maximum number of cycles required on any data point, then we can apply Inequality (1). Let the value of the function be stored in b_s bits of storage. Then, the binary signal which normally terminates a computation by turning off the clock can be used as an input to b_s *and* gates which transfer the value of the function to auxiliary storage. (Here we assume that these b_s bits always fall in the same positions in computer memory in the original machine.) With these modifications and with the addition of only b_s elements from Ω, we have constructed a sequential machine which has canonical form and runs T_{max} cycles on all inputs.

Proposition 1. *Let S be a sequential machine which computes a finite function $f(\ )$ which is such that each point of its range can be represented with b_s binary digits. Let S be constructed with 2-input binary logic elements and binary memory cells and let X be the number of logic elements it contains. Suppose that T_{max} is the maximum number of cycles required by S to compute $f(\ )$ on any point in its range. Then,*

$$(X + b_s)\, T_{max} \geqq C_\Omega(f) \tag{2}$$

We see that Inequality (2) is very close to Inequality (1) for a single machine when b_s is small relative to X. It should be noted that Inequality (2) only limits the size of T_{max} and does not limit the average number of cycles (which in fact may be a more important quantity). One can argue, however, that if the number of points in the domain of $f(\ )$ which require a number of cycles near T_{max} is small, then $f(\ )$ can be modified by deleting these points with a small effect on $C_\Omega(f)$. This would suggest that Inequality (2) may often hold at least approximately when T_{max} is replaced by the average number of cycles.

3. Storage Required for Autonomous Computation

Suppose that S computes $f(\ )$ and receives no external inputs, that is, all data needed to compute $f(\ )$ is part of the initial state of S. We say that S computes $f(\ )$ autonomously. Let s_0 be the initial state of S and $s_1, \cdots, s_T$ the successive states of S entered during the T cycles it executes while computing $f(\ )$ on some data point. We observe that no two of these states can be equal if $f(\ )$ is to be computed in finite time. Otherwise, the state repeated will be repeated infinitely many times.

Proposition 2. *Let S compute $f(\ )$ with no more than T_{max} cycles and let S have X logic elements from Ω and use b_s bits to specify a point in the range of $f(\ )$. Then, the number of bits of storage in S, namely, $|S|$, must satisfy*

$$|S| \geqq \log_2 (T_{max} + 1) \geqq \log_2 \left[\frac{C_\Omega(f)}{X + b_s} + 1 \right] \tag{3}$$

Proposition 3. *Let S consist of a small sequential machine which is attached to a very large random-access or tape storage which has $|S|$ words of storage each of which contains m bits. Then,*

$$(m + 1)\, |S|\, T_{max} (1 + \epsilon) \geqq C_\Omega(f) \tag{4}$$

for large $|S|$ where $\epsilon = \epsilon(|S|) > 0$.

This proposition follows from Inequality (2) and an earlier result (SPS 37-64, Vol. II, pp. 30–33) on the effective computing power of storage. The bound of Inequality (4) is stronger than that of Inequality (3) except when T_{max} is very large as could be expected since the storage assumed in Proposition 3 permits access to single m bit words at a time.

The complexity $C_\Omega(f)$ is large for most binary functions from $\{\Sigma_2\}^n$ to $\{\Sigma_2\}^q$ where $\Sigma_2 = \{0, 1\}$. In fact, it can be shown (Ref. 1, Theorem 2) that $C_\Omega(f)$ is greater than

$$C_\Omega(f) \geqq \frac{1}{2} \frac{q\, 2^n}{n + \log_2 q} (1 - \epsilon) \tag{5}$$

for most of these function for large n when $0 < \epsilon < 1$. Thus, the bound of Inequality (3) grows as $N + \log q$ when X is small and n and q are large. The bound of Inequality (4), however, has a much larger rate of growth.

4. Computation of Simple and Complex Functions

We turn next to the lower bound on computational work given by Inequality (1) and ask whether it can be reached for arbitrary functions f. We show that the bound can nearly be reached for simple and complex Boolean functions. (Every finite function is equivalent, up to isomorphism, to the direct product of Boolean functions of restricted domain.) We do not know whether the same is true for functions whose complexity is not at these extremes.

Consider the function $f_A(y) = y_1 y_2 \cdots y_n$ which is the *and* of y_1, y_2, y_n. $C_\Omega(f_A)$ is equal to $n - 1$ as we show by observing that (1) f_A is dependent on all inputs, (2) a

single logic element can reach at most two inputs, and (3) each additional element allows at most one additional input to be reached; also, f_A can be computed with exactly $n-1$ 2-input *and* gates, so $C_\Omega(f_A) = n-1$.

The work done to compute f_A with a single machine which contains X logic elements and which executes T cycles is given by $\chi = XT$. Clearly, then, the lower bound can be achieved when $T = 1$. When $T = k$, the machine shown in Fig. 1 will compute f_A and this machine contains an $l = \lceil n/k \rceil$-input[3] *and* gate, an *or* gate, and $k\lceil n/k \rceil + 1$ binary memory cells. The machine reads in the n inputs in groups of $\lceil n/k \rceil$ digits and, when n/k is not an integer, the last group will contain $k\lceil n/k \rceil - n$ entries which are 1. The number of logic elements in the machine is $X = \lceil n/k \rceil$ and the work done by it is

$$\chi = k\left\lceil \frac{n}{k} \right\rceil \geqq n-1 \tag{6}$$

with near equality for all $1 \leqq k \leqq n$, especially when k divides n.

Consider next the function $f_B(\mathbf{y}) = y_1^{c_1} y_2^{c_2} \cdots y_n^{c_n}$

[3] $\lceil x \rceil$ is the smallest integer equal to or greater than x.

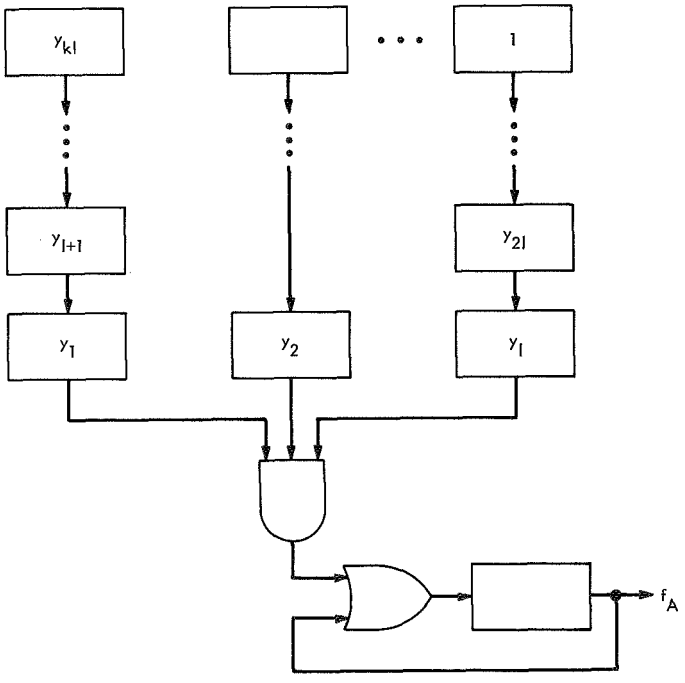

Fig. 1. Sequential machine which computes f_A

where

$$y_i^{c_i} = \begin{cases} y_i, & c_i = 0 \\ \bar{y}_i, & c_i = 0 \end{cases} \tag{7}$$

$\bar{y}_i$ is the complement of y_i and the product denotes the logical *and*. *Again* $C_\Omega(f_B) = n-1$, which follows from an argument analogous to that given above. The machine shown in Fig. 2 computes f_B in $T = k$ cycles and contains $l = \lceil n/k \rceil$ modulo-2 adders, $\lceil n/k \rceil - 1$ 2-input *and*'s, and one *or* for a total of $X = 2\lceil n/k \rceil$ logic elements. It has $2\lceil n/k \rceil + 1$ memory cells and does a work χ given by

$$\chi = 2k\left\lceil \frac{n}{k} \right\rceil \geqq n-1 \tag{8}$$

which is about a factor of 2 away from the bound when k divides n.

Clearly, the functions f_A and f_B are examples of simple functions. Now we turn to the computation of arbitrary

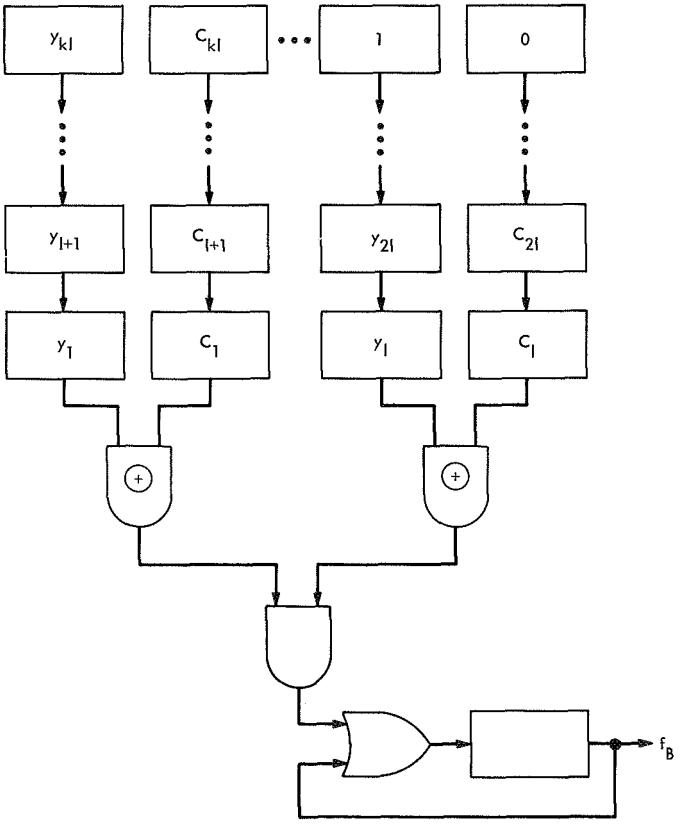

Fig. 2. Sequential machine which computes f_B

Boolean functions. (These are functions from Σ_2^n to Σ_2.) As mentioned above, the fraction of these functions for which

$$C_\Omega(f) \geqq \frac{1}{2}\frac{2^n}{n}(1-\epsilon) \tag{9}$$

where $0 < \epsilon < 1$, approaches 1 with increasing n. On the other hand, Lupanov (Ref. 2) has shown that, given $\epsilon > 0$, there exists an $N = N(\epsilon)$ such that, for $n \geqq N$, every Boolean function of n variables can be realized with

$$C_\Omega(f) \leqq \frac{2^n}{n}(1+\epsilon) \tag{10}$$

where $N(\epsilon) \to \infty$ as $\epsilon \to 0$. This means that the complexity of most Boolean functions of N variables is very large and grows nearly exponentially with N.

Any Boolean function f of n variables can be expanded as the logical *or* of minterms and the minterm $y_1^{c_1} y_2^{c_2} \cdots y_n^{c_n}$ is included if and only if f has value 1 when $y_i = \bar{c}_i$ for each $i, 1 \leqq i \leqq n$. The machine shown in Fig. 3 calculates minterms individually and successively using a stored list of all vectors $\mathbf{c} = (c_i, c_2, \cdots, c_n)$ which correspond to minterms in f. The logic unit contains n modulo-2 adders and one n-input *and* gate constructed from $n-1$ 2-input *and* gates and has one *or* gate for a total of $X = 2n$ gates. The machine executes $T = M$ cycles, where $M (\leqq 2^n)$ is the number of minterms in the function. Clearly, k copies of the minterm circuit and $k-1$ additional *or* gates could be used to compute the function in $T = \lceil m/k \rceil$ cycles. The more general machine will contain $x = 2nk + k - 1$ logic elements and do a computational work

$$\chi = [(2n+1)k - 1]\left\lceil \frac{M}{k} \right\rceil \geqq 2nM \tag{11}$$

with near equality when k divides M. Since most functions require an M near 2^{n-1}, we have that

$$\chi \simeq n2^n \tag{12}$$

for almost all Boolean functions of n variables when n is large. Comparing Inequality (12) with Inequalities (9) and (10), we find that

$$\chi \simeq n^2 C(f) \tag{13}$$

for most of these functions, and we have:

PROPOSITION 4. *Most Boolean functions f of n variables can be computed with a computational work* $\chi = XT$ *which is near the minimum required for f for all* $1 \leqq T \leqq M$ *where M is the number of minterms in the sum-of-products expansion of f.*

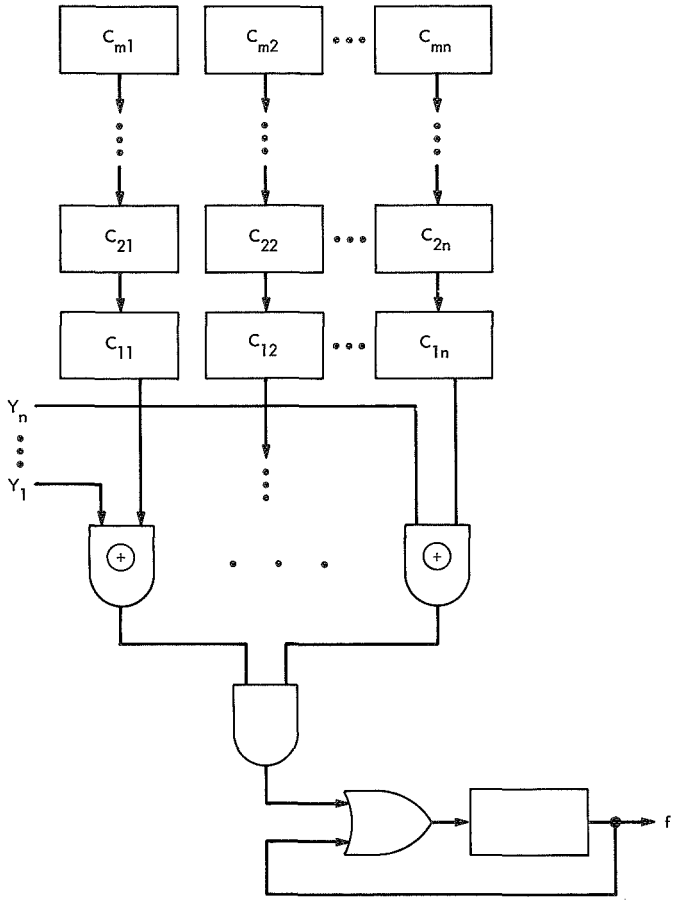

Fig. 3. Sequential machine which computes Boolean functions

It is worth noting that the number of memory cells in the above general machine is much larger than the bound of Inequality (3) but closer to Inequality (4). The storage is organized so that one word is effectively read per cycle.

5. Work Potential of a Computer

The *work potential* of a machine $\chi(t)$ is the computational work which it can do in t seconds. A machine which has X logic elements and a cycle duration D_0 has work potential

$$\chi(t) = X\frac{t}{D_0}$$

for t, a multiple of D_0. Suppose, however, that a machine has access to many types of storage with different cycle times. In particular, assume that it has a central processor

with X logic elements and cycle time D_0 and K storage units with cycle times $D_1, D_2, \cdots, D_k$ and effective computing powers $P_1, \cdots, P_k$ (the number of logic elements in an equivalent canonical machine). Then, if we order the storage units so that $D_0 \leq D_1 \leq D_2 \leq \cdots \leq D_k$, and if we assume that D_0 divides D_i, $1 \leq i \leq k$, then the work potential of the machine is given by

$$\chi(t) = t\left\{\frac{X}{D_0} + \sum_{j=1}^{J(t)} \frac{P_j}{D_j}\right\} \tag{14}$$

where $J(t)$ is such that

$$D_{J(t)} \leq t < D_{J(t)+1} \tag{15}$$

A typical plot of $\chi(t)$ is given in Fig. 4.

Many machines exist in which the slowest storage unit (such as tape) has a cycle time which is 100 to 200 times as great as the cycle time of the central processor. Since the computing power P_j is proportional to storage capacity, it is likely that P_k/D_k is much larger than X/D_0. If this is the case, the curve $\chi(t)$ will rise steeply for t near D_k and one could expect most jobs to be completed in a time near D_k if they are matched to the storage available.

The work potential rises with a slope X/D_0 if

$$P_j/D_j << X/D_0$$

so that the storage units do not improve the work potential much. On the other hand, if $P_j/D_j >> X/D_0$, the work potential may be dominated by a subset of the storage units. Since storage units are costly, a *good rule of thumb may be to choose storage units which satisfy*

$$\frac{P_j}{D_j} \simeq \frac{P_i}{D_i} \tag{16}$$

In the absence of other criteria, this rule may prove useful.

6. A Quantum-Mechanical Bound on Complexity

In this subsection, we derive a bound on the maximal complexity of any function which is computable with E ergs of energy in t seconds. Consider a sequential machine which has binary logic elements and executes T cycles to compute f. The output of each logic element can be in either of two states and the elements connected to it must make a state determination. Let the two states correspond to energy levels differing by ΔE. Then a state determination will require the consumption of at least ΔE units of energy, and the total energy E required to operate X logic elements must be at least $X\Delta E$. The duration of a cycle cannot be less than the time required for a state determination, or Δt. Then, E and the number of cycles T are bounded by

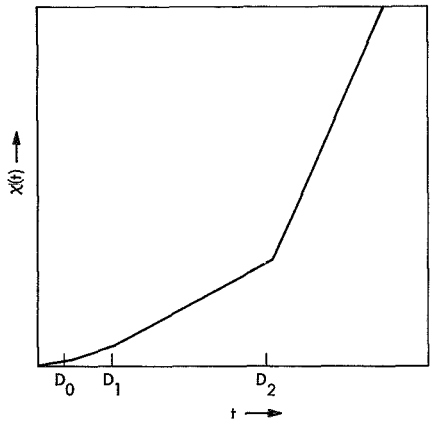

Fig. 4. Work potential

$$X \leq \frac{E}{\Delta E}\, T \leq \frac{t}{\Delta t} \tag{17}$$

where t is the number of seconds for which the machine is active. Then, the computational work of which it is capable is bounded by

$$\chi = XT \leq \frac{Et}{\Delta E \Delta t} \tag{18}$$

But the Heisenberg uncertainty relation says that measurements cannot be made unless

$$\Delta E \Delta t \geq \frac{h}{2\pi} \tag{19}$$

where h is Planck's constant with value $h = 6.624 \times 10^{-27}$ erg-second.

Therefore, function f cannot be computed by such a machine unless

$$C_\Omega(f) \leq \chi \leq \frac{(Et)\,2\pi}{h} = 0.95\,(Et)\,(\text{erg-second})^{-1}\,10^{27} \tag{20}$$

While the bound may seem to be extremely large, it is worth noting that most Boolean functions with only 110 variables cannot be computed with one erg of energy in one second. This follows from the application of the bounds of Inequalities (9) and (10).

7. A Comment on the Sorting Problem

Suppose a list of L integers from the set $\{0,1,2,\cdots,I-1\}$ is formed and we wish to order the list in the order of increasing terms. If the sorting is done in binary, a binary function with $L\lceil\log_2 I\rceil$ binary inputs and the same number of outputs will define the sorting. Consider the first sorted digit. It could be any one of the digits on the original list, so we deduce that the first output is a function of all $L\lceil\log_2 I\rceil$ inputs. Consequently,

$$C_\Omega(f) \geqq L\lceil\log_2 I\rceil - 1$$

if 2-input binary logic elements are used. This implies that the computational work required to sort must grow at least linearly with L. If no overlap exists between the circuits used to compute the $L\lceil\log_2 I\rceil$ outputs, then $C_\Omega(f)$ will grow as the square of L.

There are sorting procedures for two tape machines which sort in a number of cycles proportional to L. The effective computing power of these storage units is proportional to L, so the work done is proportional to L^2.

8. Conclusions

Six topics tied together by their relation to computational work have been discussed. One should interpret the results presented as early contributions to a nascent computer science.

References

1. Savage, J. E., "The Complexity of Decoders—Part I: Classes of Decoding Rules," *IEEE Trans. Inform. Theory*, Vol. IT-15, No. 6, Nov. 1969.
2. Lupanov, O. B., "A Method of Circuit Synthesis," *Z. zv. Vysshikh Uchebn. Zavedenii, Radiofiz*, No. 1, 1958.

C. Communication Statistics: Finite-Sample Quantile Estimation, *I. Eisenberger*

1. Introduction

Asymptotically optimum, unbiased estimators of the unknown mean μ and unknown standard deviation σ of a normal distribution using k sample quantiles are derived in Ref. 1 and given there in Tables 1 and 2 for $k = 2, 4, 6, \cdots, 20$. The asymptotic efficiency of the estimators relative to the best estimators using all the sample values are also given. However, since sample sizes are never infinite, the question arises as to the usefulness of the estimators for moderate values of the sample size n. The purpose of this article, therefore, is to give the exact moments of the sample quantiles used in estimating μ and σ for $k \leqq 6$ and $n = 50, 100, 200$. The expected value of the estimators of σ and the estimator of μ using one quantile will also be given, as well as the efficiency of all the estimators considered. Due to the symmetry of the normal density and the use of pairs of symmetric quantiles in estimating μ for $k > 1$, the estimators of μ are unbiased for $k > 1$.

2. The Asymptotic and Exact Distribution of Sample Quantiles

To define a quantile, consider a sample of n independent sample values $x_1, x_2, \cdots, x_n$ taken from a distribution of a continuous type with distribution function $F(x)$ and density function $f(x)$. The quantile of order p of the distribution or population, denoted by $\zeta(p)$, is defined as the root of the equation $F(\zeta) = p$, that is,

$$p = \int_{-\infty}^{\zeta(p)} f(x)\,dx$$

The corresponding sample quantile $z(p)$ is defined as follows. If the sample values are arranged in non-decreasing order of magnitude,

$$x_{(1)} \leqq x_{(2)} \leqq \cdots \leqq x_{(n)}$$

then $x_{(i)}$ is called the ith order statistic and

$$z(p) = x_{[np]+1}$$

where $[np]$ denotes the greatest integer $\leqq np$.

If $f(x)$ is differentiable in some neighborhood of each quantile value, it has been shown (Ref. 2) that the joint distribution of any number of quantiles is asymptotically

normal as $n \to \infty$ and that, asymptotically,

$$E(z(p)) = \zeta(p)$$

$$\mathrm{Var}(z(p)) = \frac{p(1-p)}{nf^2(\zeta(p))}$$

$$\rho_{12} = \left[\frac{p_1(1-p_2)}{p_2(1-p_1)}\right]^{1/2}$$

where ρ_{12} is the correlation between $z(p_1)$ and $z(p_2)$, $p_1 < p_2$.

Now let $g_1(x)$ denote the exact density function of the sample quantile z_1 of order p_1 and let $g_2(y)$ denote the exact density function of the sample quantile z_2 of order p_2, $p_1 < p_2$. Let $\mu_1 = [np_1]$ and let $\mu_2 = [np_2]$. Then it is also shown in Ref. 2 that $g_1(x)$ and $g_2(y)$ are given by

$$\left.\begin{aligned} g_1(x) &= \binom{n}{\mu_1}(n-\mu_1)[F(x)]^{\mu_1}[1-F(x)]^{n-\mu_1-1}f(x), \quad -\infty < x < \infty \\ g_2(y) &= \binom{n}{\mu_2}(n-\mu_2)[F(y)]^{\mu_2}[1-F(y)]^{n-\mu_2-1}f(y), \quad -\infty < y < \infty \end{aligned}\right\} \tag{1}$$

The joint density $g(x, y)$ of z_1 and z_2, which is needed in order to compute the variance of the estimators, will now be derived. The joint probability that z_1 is situated in an interval $(x, x + dx)$ and z_2 is situated in an interval $(y, y + dy)$ is identical with the probability that, among the n sample values, μ_1 are $< x$, $n - \mu_2 - 1$ are $> y + dy$, $\mu_2 - \mu_1 - 1$ are between $x + dx$ and y, one falls between x and $x + dx$, while the remaining value falls between y and $y + dy$.

Hence, since the observations are independent,

$$g(x,y) = 2\binom{n}{\mu_1}\binom{n-\mu_1}{n-\mu_2-1}\binom{\mu_2-\mu_1+1}{\mu_2-\mu_1-1}[F(x)]^{\mu_1}[1-F(y)]^{n-\mu_2-1}[F(y)-F(x)]^{\mu_2-\mu_1-1}f(x)f(y),$$

$$-\infty < x < \infty \ , \ x < y < \infty \tag{2}$$

3. The Quantile Estimators of μ and σ

The estimators of μ for $k > 1$, as given in Table 1 of Ref. 1, are of the form

$$\hat{\mu} = \sum_{i=1}^{k/2} a_i \left[z(p_i) + z(p_{k-i+1}) \right]$$

where

$$p_i < p_j \qquad \text{if } i < j$$

$$p_i = 1 - p_{k-i+1}$$

and

$$\sum_{i=1}^{k/2} a_i = 0.5$$

This means that μ is a linear combination of pairs of symmetric quantiles such that, for any choice of the p_i and coefficients a_i which satisfies the above conditions, $E(\hat{\mu}) = \mu$. However, for each value of k, the orders of the quantiles and the values of the a_i were chosen so as to minimize the asymptotic variance of $\hat{\mu}$. For $k = 1$, the asymptotically unbiased estimator of μ is given by

$$\hat{\mu} = z(0.5)$$

In all cases, the efficiency of $\hat{\mu}$ was defined as

$$\mathrm{Eff}(\hat{\mu}) = \frac{\sigma^2}{n\,\mathrm{Var}(\hat{\mu})} \tag{3}$$

The estimators of σ in Table 2 of Ref. 1 are also linear combinations of pairs of symmetric quantiles of the form

$$\hat{\sigma} = \sum_{i=1}^{k/2} b_i \left[z(p_{k-i+1}) - z(p_i) \right]$$

where the orders of the quantiles and the coefficients b_i were chosen so as to satisfy simultaneously the conditions that $\hat{\sigma}$ be asymptotically unbiased and that the asymptotic

variance of σ be a minimum. The efficiency of σ was defined as

$$\text{Eff}(\hat{\sigma}) = \frac{\sigma^2}{2n \operatorname{Var}(\hat{\sigma})} \tag{4}$$

4. Exact Moments of the Quantiles and Estimators

Using Eq. (1), the means and variances of the quantiles used in estimating μ and σ for the cases under consideration were computed for $n = 50, 100$, and 200 and are given in Table 1. Since

$$E(z(p)) - \mu = -[E(z(1-p)) - \mu]$$

and

$$\operatorname{Var}(z(p)) = \operatorname{Var}(z(1-p))$$

the results for $k > 1$ are given only for $i \leqq k/2$.

Using Eq. (2) and the results previously obtained, the exact correlations between $z(p_i)$ and $z(p_j)$ were computed and are given, along with the asymptotic values, in Table 2.

The normalized expected values of the estimators of σ were computed and are given in Table 3. The asymptotic values are, of course, equal to one for all k. The normalized bias of the estimator of μ using one quantile is shown in Table 1 as $[E(zp) - \mu]/\sigma$ for $k = 1$.

The variances of the estimators of μ and σ were computed and, by means of Eqs. (3) and (4), the efficiencies of the estimators were determined and are also given in Table 3.

The results of this investigation indicate that even for moderate values of n, the quantile estimators of the unknown parameters of a normal population, although derived on the basis of the asymptotic distribution and moments of the quantiles, can be useful.

References

1. Eisenberger, I., and Posner, E. C., "Systematic Statistics Used for Data Compression in Space Telemetry," *J. Am. Statist. Assoc.*, Vol. 60, pp. 97–133, Mar. 1965. Also, Technical Report 32-510, Jet Propulsion Laboratory, Pasadena, Calif., Oct. 1, 1963.
2. Cramer, H., *Mathematical Methods of Statistics*. Princeton University Press, Princeton, N.J., 1946.

Table 1. Asymptotic and exact moments of the quantiles used to estimate μ and σ for $k = 1, 2, 4, 6$ and $n = 50, 100, 200$

k	p	Asymptotic		$n = 200$		$n = 100$		$n = 50$	
		$\frac{E(z(p)) - \mu}{\sigma}$	$\frac{n \operatorname{Var}(z(p))}{\sigma^2}$	$\frac{E(z(p)) - \mu}{\sigma}$	$\frac{n \operatorname{Var}(z(p))}{\sigma^2}$	$\frac{E(z(p)) - \mu}{\sigma}$	$\frac{n \operatorname{Var}(z(p))}{\sigma^2}$	$\frac{E z(p)) - \mu}{\sigma}$	$\frac{n \operatorname{Var}(z(p))}{\sigma^2}$
For estimating μ									
1	0.5	0	1.5708	0.00625	1.5657	0.0125	1.5622	0.0249	1.5556
2	0.2709	−0.610	1.8007	−0.605	1.7945	−0.596	1.7816	−0.610	1.7827
4	0.1068	−1.244	2.8170	−1.238	2.8080	−1.249	2.8255	−1.218	2.7136
	0.3512	−0.382	1.6567	−0.378	1.6512	−0.371	1.6434	−0.384	1.6412
6	0.0540	−1.607	4.2465	−1.617	4.3560	−1.591	4.1423	−1.628	4.2930
	0.1915	−0.872	2.0824	−0.868	2.0779	−0.857	2.0539	−0.873	2.0621
	0.3898	−0.280	1.6163	−0.285	1.6138	−0.292	1.6117	−0.278	1.6000
For estimating σ									
2	0.0694	−1.483	3.6599	−1.492	3.7205	−1.507	3.7641	−1.463	3.5044
4	0.0230	−1.995	7.5562	−1.997	7.7199	−1.946	6.8769	−1.855	5.8242
	0.1271	−1.140	2.5568	−1.137	2.5578	−1.147	2.5669	−1.119	2.4833
6	0.0104	−2.312	13.5558	−2.229	11.5449	−2.148	9.5767	−2.248	10.7783
	0.0548	−1.600	4.2100	−1.617	4.3800	−1.591	4.1470	−1.627	4.2964
	0.1696	−0.956	2.2062	−0.963	2.2240	−0.971	2.2256	−0.049	2.1719

Table 2. Asymptotic and exact values of the correlation between the quantiles used to estimate μ and σ for $k = 2, 4, 6$ and $n = 50, 100, 200$

k	Correlation	$\hat{\mu}$				$\hat{\sigma}$			
		Asymptotic values	Exact values			Asymptotic values	Exact values		
			$n = 200$	$n = 100$	$n = 50$		$n = 200$	$n = 100$	$n = 50$
2	ρ_{12}	0.3716	0.3746	0.3812	0.3743	0.0748	0.0714	0.0695	0.0787
4	ρ_{14}	0.1196	0.1203	0.1180	0.1274	0.0235	0.0228	0.0270	0.0346
	ρ_{23}	0.5413	0.5446	0.5522	0.5427	0.1456	0.1457	0.1437	0.1533
	$\rho_{12} = \rho_{34}$	0.4700	0.4696	0.4627	0.4855	0.4021	0.3920	0.4301	0.4757
	$\rho_{13} = \rho_{24}$	0.2544	0.2559	0.2554	0.2631	0.0585	0.0577	0.0623	0.0728
6	ρ_{16}	0.0571	0.0547	0.0594	0.0554	0.0105	0.0130	0.0169	0.0141
	ρ_{25}	0.2367	0.2381	0.2439	0.2386	0.0580	0.0542	0.0592	0.0553
	ρ_{34}	0.6383	0.6324	0.6271	0.6432	0.2042	0.2001	0.1982	0.2089
	$\rho_{12} = \rho_{56}$	0.4909	0.4768	0.4927	0.4820	0.4258	0.4753	0.5271	0.4922
	$\rho_{13} = \rho_{46}$	0.2989	0.2938	0.3076	0.2945	0.2268	0.2549	0.2899	0.2610
	$\rho_{14} = \rho_{36}$	0.1920	0.1862	0.1930	0.1890	0.0463	0.0515	0.0578	0.0434
	$\rho_{15} = \rho_{26}$	0.1163	0.1141	0.1203	0.1150	0.0247	0.0267	0.0316	0.0280
	$\rho_{23} = \rho_{45}$	0.6089	0.6126	0.6231	0.6094	0.5328	0.5148	0.5423	0.5146
	$\rho_{24} = \rho_{35}$	0.3890	0.3880	0.3912	0.3919	0.1088	0.1042	0.1003	0.1077

Table 3. The normalized expected value of the estimators of σ and the asymptotic and exact efficiencies of the estimators of μ and σ for $n = 50, 100, 200$

k	$E(\hat{\sigma})/\sigma$			Asymptotic		$n = 200$		$n = 100$		$n = 50$	
	$n = 200$	$n = 100$	$n = 50$	Eff $(\hat{\mu})$	Eff $(\hat{\sigma})$	Eff $(\hat{\mu})$	Eff $(\hat{\sigma})$	Eff $(\hat{\mu})$	Eff $(\hat{\sigma})$	Eff $(\hat{\mu})$	Eff $(\hat{\sigma})$
1				0.6366		0.6387		0.6401		0.6428	
2	1.0068	1.0169	0.9872	0.8098	0.6522	0.8108	0.6388	0.8126	0.6270	0.8164	0.6801
4	1.0000	0.9929	0.9585	0.9201	0.8244	0.9215	0.8208	0.9234	0.8415	0.9263	0.9035
6	0.9985	0.9861	0.9980	0.9560	0.8943	0.9582	0.8925	0.9596	0.9184	0.9615	0.9165

D. Frequency Generation and Control: Analysis of Random Modulation in Amplifier Circuits,

A. Sward and G. Thompson

1. Introduction

The growing demand for more stable frequency sources has been answered in part with the advent of the hydrogen maser frequency standard. The requirements for the frequency standard and some preliminary data are described in SPS 37-59, Vol. II, pp. 40–43. This demand for stability has imposed a number of stringent requirements upon the phase noise and phase stability of receivers for the Deep Space Network. Therefore, much effort has been put into analyzing and minimizing phase noise in RF communication equipment.

Until recently, it was difficult to make low-level phase noise measurements. Phase jitter measurements were restricted to voltage-controlled oscillators, frequency synthesizers, etc., where phase jitter was high. However, the availability of more sensitive measuring equipment has enabled better measurements to be made (SPS 37-64, Vol. II, pp. 55–59).

In general, a sinusoidal carrier may be subjected to either of two kinds of modulation, angle modulation and

amplitude modulation. Consider a carrier signal $x(t)$ modulated by the low-frequency processes $A(t)$ and $\phi(t)$.

$$x(t) = [1 + A(t)] \cos [\omega_0 t + \phi(t)] \tag{1}$$

Since $A(t)$ and $\phi(t)$ are low-frequency random processes, the effect upon $x(t)$ is a broadening or degradation of the spectrum. The question, however, is to what extent each of the two types of noise contributes to the broadening of the spectrum.

In this article, a theoretical basis for meaningful amplitude-modulation (AM) and phase-modulation (PM) measurements is developed. In the circuits encountered in a receiver (amplifiers, frequency multipliers, dividers, etc.), the dominant AM and PM noise processes have a power spectral density with a $1/f$ behavior. To compare the performance of one circuit relative to another, a measure $\mathcal{J}$ of the power in the AM and PM processes is defined. The goals for the circuit design can be seen from the functional behavior of $\mathcal{J}$.

2. General Theory

Consider the complex signal $x_c(t)$ of the form

$$x_c(t) = [1 + A(t)] \exp [j\omega_0 t + j\phi(t)] \tag{2}$$

where ω_0 is the frequency and where $A(t)$ and $\phi(t)$ represent random amplitude and phase modulation, respectively. The functions $A(t)$ and $\phi(t)$ are assumed to be independent, zero-mean, baseband random processes.

The autocorrelation function $R_{x_c}(\tau)$ of $x_c(t)$ is defined to be (Ref. 1, p. 37)

$$R_{x_c}(\tau) = \langle x_c(t + \tau) x_c^*(t) \rangle \tag{3}$$

where the asterisk (*) denotes the complex conjugate and the brackets $\langle\ \rangle$ denote an ensemble average. Substituting Eq. (2) into this expression and using the fact that $A(t)$ and $\phi(t)$ are independent, one finds that

$$R_{x_c}(\tau) = \langle [1 + A(t + \tau)] [1 + A(t)] \rangle \times \langle \exp [j\phi(t + \tau) - j\phi(t)] \rangle \exp (j\omega_0 \tau) \tag{4}$$

The first ensemble average in Eq. (4) can be written in terms of the autocorrelation $R_A(\tau)$ of $A(t)$ as

$$\langle [1 + A(t + \tau)] [1 + A(t)] \rangle = 1 + R_A(\tau) \tag{5}$$

By defining the low-frequency process $m(t)$ as

$$m(t) = \exp [j\phi(t)] \tag{6}$$

the second ensemble average in Eq. (4) can be written

$$R_m(\tau) = \langle \exp [j\phi(t + \tau) - j\phi(t)] \rangle \tag{7}$$

where $R_m(\tau)$ is the autocorrelation function of $m(t)$. One can now express $R_{x_c}(\tau)$ in terms of $R_A(\tau)$ and $R_m(\tau)$ as

$$R_{x_c}(\tau) = [1 + R_A(\tau)] R_m(\tau) \exp (j\omega_0 \tau) \tag{8}$$

In amplifiers, the phase-modulation process $\phi(t)$ has been observed experimentally (SPS 37-64, Vol. II) to have a small magnitude ($|\phi(t)| << 1$). For processes with finite power, such as the model for $1/f$ noise given in *Subsection 3*, Eq. (6) can be approximated by (Ref. 1, p. 123)

$$m(t) \approx 1 + j\phi(t) - \frac{\phi^2(t)}{2}$$

The autocorrelation $R_m(\tau)$ is then approximately

$$R_m(\tau) \approx 1 - R_\phi(0) + R_\phi(\tau)$$

where $R_\phi(\tau)$ is the autocorrelation function of $\phi(t)$. Hence, Eq. (8) can be written

$$R_{x_c}(\tau) \approx [1 + R_A(\tau)] [1 - R_\phi(0) + R_\phi(\tau)] \exp (j\omega_0 \tau) \tag{9}$$

The narrowband function of primary interest is the real part of $x_c(t)$ given by $x(t)$, as in Eq. (1),

$$\left.\begin{aligned} x(t) &= Re [x_c(t)] \\ x(t) &= [1 + A(t)] \cos [\omega_0 t + \phi(t)] \end{aligned}\right\} \tag{10}$$

which has the autocorrelation function $R_x(\tau)$ given by (Ref. 1, p. 110)

$$R_x(\tau) = \frac{1}{2} Re [R_{x_c}(\tau)]$$

From Eq. (9),

$$R_x(\tau) = \frac{1}{2} [1 + R_A(\tau)] [1 - R_\phi(0) + R_\phi(\tau)] \cos \omega_0 \tau \tag{11}$$

This is the time-domain result that was to be obtained. The second-order statistics of $x(t)$ are related to the second-order statistics of $A(t)$ and $\phi(t)$ through Eq. (11).

The Fourier transform of $R_x(\tau)$ is the power spectral density $S_x(\omega)$ of $x(t)$ given by (Ref. 2, p. 1)

$$S_x(\omega) = \int_{-\infty}^{\infty} R_x(\tau)\, e^{-j\omega\tau}\, d\tau$$

Applying this transformation to Eq. (11) and using well-known properties of the Fourier integral (Ref. 2, Chap. 2 and 3), one obtains

$$S_x(\omega) = \frac{1}{4}\{2\pi\,[1 - R_\phi(0)]\,\delta(\omega) + S_\phi(\omega) + [1 - R_\phi(0)]\,S_A(\omega) + \frac{1}{2\pi}\,S_A(\omega) \circledast S_\phi(\omega)\} \times \circledast\,[\delta(\omega - \omega_0) + \delta(\omega + \omega_0)] \tag{12}$$

where $S_A(\omega)$ and $S_\phi(\omega)$ are the spectral densities of $A(t)$ and $\phi(t)$, respectively, and where $\circledast$ denotes the convolution operator [Ref. 2, p. 27]. From Eq. (12), one can see that the signal $x(t)$ is the sum of a discrete carrier component with power P_c given by

$$P_c = \frac{1}{2}\,[1 - R_\phi(0)] \tag{13}$$

and three sideband components which are the result of the amplitude and phase modulation. Note that if either $S_A(\omega)$ or $S_\phi(\omega)$ is identically zero, Eq. (12) reduces to the form of linear-phase or amplitude modulation, respectively. The primary restriction on the validity of Eq. (12) is that it applies to the case of low-power phase modulation ($|\phi(t)| << 1$).

3. Application to 1/f Noise

In the frequency synthesis and distribution circuits considered here, the power spectra of $A(t)$ and $\phi(t)$ have been found empirically (SPS 37-64, Vol. II) to have the form of $1/f$ noise. The model for these spectra is taken to be

$$S_A(\omega) = \begin{cases} \dfrac{b_A^2}{|\omega| + a} & \text{for } |\omega| \leq c \\ 0 & \text{for } |\omega| > c \end{cases} \tag{14}$$

and

$$S_\phi(\omega) = \begin{cases} \dfrac{b_\phi^2}{|\omega| + a} & \text{for } |\omega| \leq c \\ 0 & \text{for } |\omega| > c \end{cases} \tag{15}$$

where c is the effective 3-dB frequency of the narrowband circuit, where a $<<1$ is a constant, and where b_A and b_ϕ are empirically determined constants. The spectra are arbitrarily assumed to be zero for $|\omega| > c$, but this should have negligible effect on the results as long as the response of the circuit falls off faster than $1/f$ as $f \to \infty$. The parameter $a/2\pi$ is a very small number less than one cycle per year (Ref. 3) which has yet to be measured experimentally. For this reason, a is the same in both $S_A(\omega)$ and $S_\phi(\omega)$, and its actual value has little effect on the results to be obtained.

In Eq. (12), the convolution of $S_A(\omega)$ and $S_\phi(\omega)$ is one of the components of sideband modulation. Let $S_{AX\phi}(\omega)$ be the cross term between $A(t)$ and $\phi(t)$ so that (Ref. 2, p. 27)

$$S_{AX\phi}(\omega) = \frac{1}{2\pi}\int_{-\infty}^{\infty} S_A(\xi)\, S_\phi(\omega - \xi)\, d\xi \tag{16}$$

Using the particular spectra in Eqs. (14) and (15), one can find that

$$S_{AX\phi}(0) = \frac{b_A^2\, b_\phi^2\, c}{\pi\, a\,(c + a)} \tag{17a}$$

$$S_{AX\phi}(\omega) = \frac{b_A^2\, b_\phi^2}{\pi}\,\frac{1}{\omega}\ln\frac{(\omega + a)\,(c - \omega + a)}{a\,(c + a)} + \frac{1}{\omega + 2a}\ln\frac{(\omega + a)}{a}, \qquad 0 < |\omega| \leq c \tag{17b}$$

$$S_{AX\phi}(\omega) = \frac{b_A^2\, b_\phi^2}{\pi}\,\frac{1}{\omega + 2a}\ln\frac{(c + a)}{(\omega - c + a)}, \qquad c < |\omega| \leq 2c \tag{17c}$$

$$S_{AX\phi}(\omega) = 0, \qquad 2c < |\omega| < \infty \tag{17d}$$

For the case of simultaneous amplitude and phase modulation with $1/f$ noise, the spectrum of the carrier signal is given by Eqs. (12), (14), (15), and (17).

4. The Comparative Measure $\mathcal{J}(\omega_1, \omega_2)$

In evaluating the amount of signal degradation produced by a circuit, some measure of the energy loss from the carrier to the sidebands is needed. Often spectral broadening of the carrier is important, but for the low-index modulation above, the broadening is of the order of 10^{-8} Hz, which cannot be resolved. Contrary to the random walk of the phase of an oscillator, the phase deviation of an amplifier cannot increase without bound because it is limited by the phase transfer characteristic of the amplifier. Of greater interest is a measure of the amount of sideband power to carrier power. For phase modulation alone, such a measure has been defined (Ref. 4). Another measure $\mathcal{J}(\omega_1, \omega_2)$ can be defined for the more general case of both amplitude and phase modulation as

$$\mathcal{J}(\omega_1, \omega_2) \equiv \frac{\text{single sideband power for } |\omega| \in [\omega_1, \omega_2]}{\text{total carrier power}} \tag{18}$$

per device, referred to the input. Since $1/f$ noise is the predominant spectral shape considered here, then, for $a << \omega_1 < \omega_2 << c$, $\mathcal{J}(\omega_1, \omega_2)$ will indicate the relative level of the modulation spectrum independently of a and c. This property can be seen by evaluating $\mathcal{J}(\omega_1, \omega_2)$ for the spectra of Eqs. (14) and (15).

Substituting the sideband and carrier components from Eq. (12) into Eq. (18) yields

$$\mathcal{J}(\omega_1, \omega_2) = \frac{\frac{1}{4\pi}\int_{\omega_1}^{\omega_2} \{S_\phi(\omega) + [1 - R_\phi(0)]\, S_A(\omega) + S_{AX\phi}(\omega)\}\, d\omega}{P_c} \tag{19}$$

where P_c is given by Eq. (13). From Eq. (17b), in the range $a << |\omega| << c$, $S_{AX\phi}(\omega)$ can be approximated by

$$S_{AX\phi}(\omega) \approx \frac{2b_A^2 b_\phi^2}{\pi}\frac{1}{\omega}\ln\frac{\omega}{a}, \qquad a << |\omega| << c$$

By using this approximation in Eq. (19), one can find that

$$\mathcal{J}(\omega_1, \omega_2) = \frac{(b_A^2 + b_\phi^2)\ln\frac{(\omega_2 + a)}{(\omega_1 + a)} + \frac{b_A^2 b_\phi^2}{\pi}\left[\ln\frac{\omega_1\omega_2}{a^2}\ln\frac{\omega_2}{\omega_1} - \ln\frac{(c+a)}{a}\ln\frac{(\omega_2+a)}{(\omega_1+a)}\right]}{2\pi\left[1 - \frac{b_\phi^2}{\pi}\ln\frac{(c+a)}{a}\right]}$$

The approximation that $a << \omega_1 < \omega_2 << c$ still holds so that

$$\mathcal{J}(\omega_1, \omega_2) \approx \ln\frac{\omega_2}{\omega_1}\,\frac{b_A^2 + b_\phi^2 + \frac{b_A^2 b_\phi^2}{\pi}\ln\frac{\omega_1\omega_2}{ca}}{2\pi\left(1 - \frac{b_\phi^2}{\pi}\ln\frac{c}{a}\right)} \tag{20}$$

The parameter a is not known so that one must estimate the relative sizes of the terms in Eq. (20). Experimentally (SPS 37-64, Vol. II), b_A^2 and b_ϕ^2 in Eq. (20) are on the order of 10^{-6}. For an amplifier bandwidth $c/2\pi = 10^6$Hz, one would have to observe the amplifier output for 10^{10^6} yr before the last terms in the numerator and denominator of Eq. (20) would be comparable to the first terms. Hence, Eq. (20) can be approximated as

$$\mathcal{J}(\omega_1, \omega_2) \approx \frac{1}{2\pi}(b_A^2 + b_\phi^2)\ln\frac{\omega_2}{\omega_1} \tag{21}$$

The approximation made in obtaining Eq. (21) from Eq. (20) should be checked when applying these results to a particular circuit.

The measure $\mathcal{J}(\omega_1, \omega_2)$ includes the effects of both amplitude and phase modulation. In practice, one often wishes to know the relative contributions of the two types of modulation. Hence, additional measures, $\mathcal{A}(\omega_1, \omega_2)$ for

amplitude modulation and $\mathcal{P}(\omega_1, \omega_2)$ for phase modulation (Ref. 4), are useful. For amplitude modulation alone define

$$\mathcal{A}(\omega_1, \omega_2) \equiv \frac{\text{single sideband AM power for } |\omega| \in [\omega_1, \omega_2]}{\text{total carrier power}} \tag{22}$$

per device, referred to the input. The carrier function that is amplitude-modulated only is given by $x(t)$ in Eq. (10) with $\phi(t) \equiv 0$. In this case, the spectral density is given by Eq. (12) with $S_\phi(\omega) \equiv 0$ so that $\mathcal{A}(\omega_1, \omega_2)$ can be expressed as

$$\mathcal{A}(\omega_1, \omega_2) = \frac{\frac{1}{4\pi}\int_{\omega_1}^{\omega_2} S_A(\omega)\, d\omega}{P_c}$$

where the carrier power P_c is given by Eq. (13) with $R_\phi(0) = 0$. Evaluating the above function for the $1/f$ spectrum of Eq. (14), one obtains

$$\mathcal{A}(\omega_1, \omega_2) = \frac{b_A^2}{2\pi} \ln \frac{(\omega_2 + a)}{(\omega_1 + a)} \tag{23}$$

Similarly, for phase modulation alone define (Ref. 4)

$$\mathcal{P}(\omega_1, \omega_2) \equiv \frac{\text{single sideband PM power for } |\omega| \in [\omega_1, \omega_2]}{\text{total carrier power}} \tag{24}$$

per device, referred to the input. When $A(t) \equiv 0$ in Eq. (10), then $S_A(\omega) \equiv 0$ in Eq. (12) so that

$$\mathcal{P}(\omega_1, \omega_2) = \frac{\frac{1}{4\pi}\int_{\omega_1}^{\omega_2} S_\phi(\omega)\, d\omega}{\frac{1}{2}[1 - R_\phi(0)]}$$

Evaluating this expression for the $S_\phi(\omega)$ in Eq. (15) and assuming $R_\phi(0) << 1$, one finds

$$\mathcal{P}(\omega_1, \omega_2) = \frac{b_\phi^2}{2\pi} \ln \frac{(\omega_2 + a)}{(\omega_1 + a)} \tag{25}$$

Comparing Eqs. (21), (23), and (25) and assuming $a << \omega_1 < \omega_2$, then one can write

$$\mathcal{J}(\omega_1, \omega_2) \approx \mathcal{A}(\omega_1, \omega_2) + \mathcal{P}(\omega_1, \omega_2) \tag{26}$$

This relationship implies that when the AM and the PM are both small, then the modulation processes can be handled separately.

5. Application to Circuit Design

A plot of Eq. (26) is given in Fig. 1. The design goal for a circuit should be clear from this plot. For a given value of $\mathcal{A}$, one should make $\mathcal{P} \approx \mathcal{A}$ to obtain nearly the lowest amount of signal degradation due to amplitude and phase modulation. Further reductions of $\mathcal{P}$ can realize at most a 3-dB improvement in $\mathcal{J}$. Obviously both $\mathcal{A}$ and $\mathcal{P}$ should be made as small as possible.

In practice, comparisons using the above ideas are very simple. If one standardizes on a 1-Hz bandwidth at 10 Hz, then a measurement of the power or rms voltage in this bandwidth can serve as a basis for the comparison of circuit performance. Detailed measurements and measurement techniques are presented in SPS 37-64, Vol. II.

6. Conclusions

This article has shown that random modulation of the amplitude and phase of a sinusoidal carrier produces sideband components which degrade the spectral characteristics of the ideal carrier. A measure of this degradation is given by the sideband to carrier power ratio $\mathcal{J}$ defined in Eq. (20). Evaluation of $\mathcal{J}$ in Eq. (23) for AM and PM by $1/f$ noise spectra shows that the two noise components

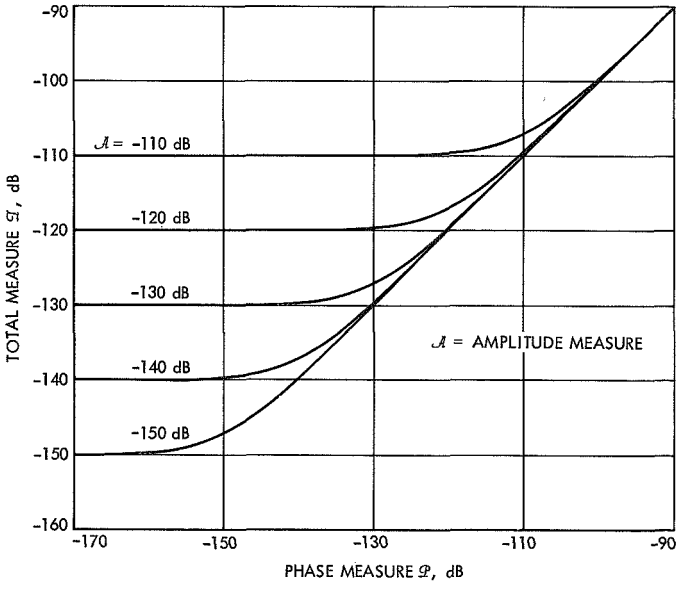

Fig. 1. Relative contributions of amplitude and phase noise to single sideband power

affect $\mathcal{J}$ symmetrically. The value of $\mathcal{J}$ is effectively minimized by making the AM and PM contributions equal and as small as possible.

References

1. Rowe, H. E., *Signals and Noise in Communication Systems.* D. Van Nostrand Co., Inc., Princeton, N.J., 1965.
2. Papoulis, A., *The Fourier Integral and Its Applications.* McGraw-Hill Book Co., Inc., New York, 1962.
3. Atkinson, W. R., Fey, R. L., and Newman, J., "Spectrum Analysis of Extremely Low Frequency Variations of Quartz Oscillators," *Proceedings of the IEEE,* Vol. 51, p. 379, Feb. 1963.
4. Halford, D., *Phase Noise of RF Amplifiers and Frequency Multipliers,* U.S. Government Memorandum 253.04. National Bureau of Standards, Boulder, Colorado, Oct. 25, 1967.

E. Frequency Generation and Control: Angle Demodulation Using State-Variable Techniques, *G. Thompson*

1. Introduction

Space communication systems typically use a sinusoidal carrier that is phase-modulated by a multitude of signals such as engineering and scientific data, command and control information, and integrated doppler frequency shift. Analyses of such systems generally require a large number of simplifying assumptions in order to obtain a tractable receiver design (SPS 37-58, Vol. III, pp. 42–50, and SPS 37-60, Vol. III, pp. 46–56). The purpose of this article is to formulate the problem using the state-variable approach, which enables one to design a receiver system and to predict its performance in a straightforward manner.

A fairly general form for the signal $g(t)$ detected by a space communications receiver is (SPS 37-58, Vol. III, pp. 42–50)

$$g(t) = (2P_s)^{1/2} \times \sin\left[\omega_0 t + \int_0^t w_d(\tau)\, d\tau + \sum_{k=1}^{K} s_k(t) \cos \omega_k t + \theta_0\right] \quad (1)$$

where

P_s = total signal power

ω_0 = nominal carrier frequency in sec^{-1}

$w_d(\tau)$ = residual doppler frequency shift

$s_k(t)$ = data signal which biphase-modulates the subcarrier $\cos \omega_k t$

θ_0 = unknown initial phase angle

The signal in Eq. (1) can be represented in the form

$$g(t) = (2P_s)^{1/2} \sin\left[\omega_0 t + H(t)\, X(t)\right] \quad (2)$$

where $H(t)$ is a $1 \times N$ row vector, and where $X(t)$ is an $N \times 1$ column vector of random processes or state variables $x_i(t)$, $i = 1, 2, \cdots, N$. The statistics of the $x_i(t)$ are chosen to model the unknown parameters and/or the random processes of the angle modulation in Eq. (1).

For signals of the form of Eq. (2), the receiver structure resulting from the state-variable approach (Ref. 1) can be significantly simplified. In *Subsection 2,* the receiver, called a nonlinear, recursive estimator (NLRE), is derived for the case where the state vector $X(t)$ can be modeled as the output of a linear system driven by white noise. The assumption that the time variations of $X(t)$ are slow compared to the carrier frequency ω_0(narrowband) allows some of the system parameters to be decoupled from the estimate of the signal. Considerable simplification of the system structure results.

At large values of signal-to-noise ratio (SNR), a linear equivalent system for the NLRE is known to be optimum in the minimum-mean-square-error (MMSE) sense. The MMSE covariance matrix for the linear system is given by the solution to a matrix Riccati equation, which also applies to the NLRE under the narrowband assumption mentioned above. Hence, the state-variable approach becomes optimum at high SNR and is sub-optimum in the vicinity of threshold. Since the state-variable approach is intended to handle large systems of random processes, the matrix formulation makes specification of system structure and evaluation of system performance straightforward.

Two examples of the application of this method to phase-modulated carrier signals are given.

2. The Nonlinear-Recursive Estimator

The $N \times 1$ vector random process $X(t)$ is assumed to be a vector Markov process (Ref. 1, p. 8) generated by the output of a linear system driven by an $R \times 1$ white-noise vector $U(t)$. The stochastic system can be represented by

$$\dot{X}(t) = A(t)X(t) + B(t)U(t) \tag{3}$$

where $A(t)$ and $B(t)$ are $N \times N$ and $N \times R$ matrices, respectively. The observable $y(t)$ is the sum of the signal $g(t)$ in Eq. (2) corrupted by additive noise $v(t)$ so that

$$y(t) = (2P_s)^{1/2} \sin[\omega_0 t + H(t)X(t)] + v(t) \tag{4}$$

The properties of the noise are given by the equations

$$E[U(t)] = 0 \tag{5a}$$

$$E[v(t)] = 0 \tag{5b}$$

$$E[U(t_1)U^T(t_2)] = K\delta(t_2 - t_1) \tag{5c}$$

$$E[v(t_1)v(t_2)] = L\delta(t_2 - t_1) \tag{5d}$$

$$E[U(t_1)v(t_2)] \equiv 0 \tag{5e}$$

where K and L are appropriately dimensioned matrices, where $\delta(\cdot)$ is the Dirac delta function, and where the superscript T indicates the matrix transpose.

The estimate $\hat{X}(t)$ of $X(t)$ is determined by a NLRE which has the form (Ref. 2, p. 180)

$$\left.\begin{aligned} \dot{\hat{X}}(t) &= A(t)\hat{X}(t) + P(t)C^T(t)L^{-1}\{y(t) - g[\hat{X}(t), t]\} \\ \hat{X}(0) &= E[X(0)] \end{aligned}\right\} \tag{6}$$

where

$$\left.\begin{aligned} \dot{P}(t) &= A(t)P(t) + P(t)A^T(t) - P(t)C^T(t)L^{-1}C(t)P(t) \\ &\quad + B(t)KB^T(t) \\ P(0) &= E\{[X(0) - X(0)][\hat{X}(0) - \hat{X}(0)]^T\} \end{aligned}\right\} \tag{7}$$

and where

$$C(t) = \left[\frac{\partial g[X(t), t]}{\partial x_i}\right]_{X=\hat{X}} \tag{8}$$

A block diagram representation of this NLRE appears in Fig. 1.

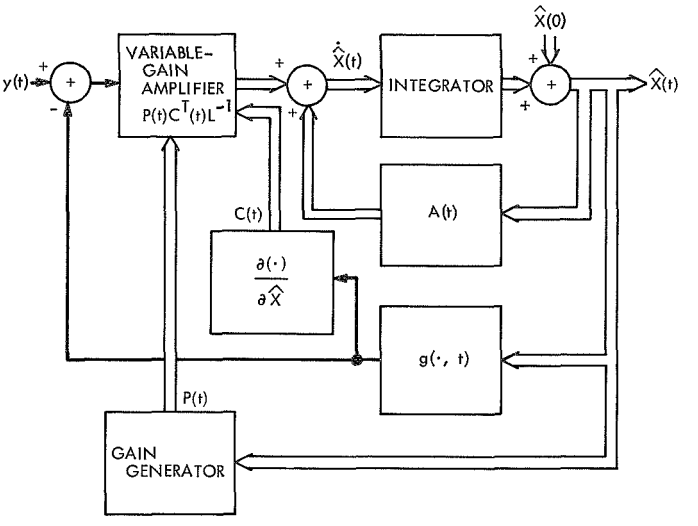

Fig. 1. Nonlinear, recursive estimator for a scalar observation

The NLRE is the result of linearizing the signal about the estimate and applying the Kalman–Bucy filtering algorithm (Ref. 2, Chap. 7). Other approximations are possible, but in practice they probably will perform similarly (Ref. 3). In this regard, further theoretical work is necessary to predict the performance of a NLRE, especially in the threshold region.

For sinusoidal signals, a narrowband assumption is often invoked (Ref. 1, p. 54), which in this case gives significant results. For $g(t)$ given by Eq. (2) then $C(t)$ in Eq. (8) is given by

$$C(t) = (2P_s)^{1/2} H(t) \cos[\omega_0 t + H(t)\hat{X}(t)] \tag{9}$$

The use of this equation in Eqs. (6) and (7) yields terms at a frequency of $2\omega_0$ which may be neglected since the remainder of the estimator is low-pass (Ref. 1, p. 54). Hence, with the narrowband assumption the NLRE has the form

$$\left.\begin{aligned} \dot{\hat{X}} &= A\hat{X} + \frac{(2P_s)^{1/2}}{L} P H^T y(t) \cos(\omega_0 t + H\hat{X}) \\ \hat{X}(0) &= E[X(0)] \end{aligned}\right\} \tag{10}$$

where

$$\left.\begin{aligned} \dot{P} &= AP + PA^T - \frac{P_s}{L} PH^T HP + BKB^T \\ P(0) &= E\{[X(0) - \hat{X}(0)][X(0) - \hat{X}(0)]^T\} \end{aligned}\right\} \tag{11}$$

The time argument has been dropped except where necessary to preserve clarity.

The simplification resulting from the narrowband assumption is evident in Fig. 2. The differencing operation $y(t) - g[\hat{X}(t), t]$ is eliminated and the system that generates the P matrix is now decoupled from the estimate $\hat{X}(t)$, which enables one to generate the P matrix before any observations are made. The validity of this approximation has been verified by simulation results (Ref. 1, p. 95). This decoupling occurs only for the case of angle modulation, which is, however, of primary interest for space communication systems. As shown in *Subsection* 3, the P matrix now represents the true error covariance matrix at large values of the SNR.

3. Linearized Model

To find a linear equivalent system for a NLRE, consider the behavior of the system without any input noise so that

$$y(t) = g(t) = (2P_s)^{1/2} \sin(\omega_0 t + HX)$$

For this case, the last term in Eq. (10) becomes

$$\frac{PC^T}{L} y(t) = \frac{2P_s}{L} PH^T \cos(\omega_0 t + H\hat{X}) \sin(\omega_0 t + HX)$$

or

$$\frac{PC^T}{L} y(t) = \frac{P_s}{L} PH^T \times \{\sin[2\omega_0 t + H(X + \hat{X})] + \sin[H(X - \hat{X})]\}$$

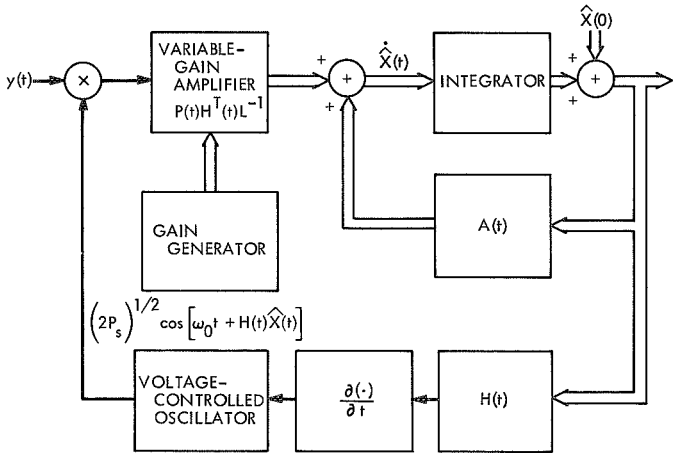

Fig. 2. NLRE using narrowband assumption for sinusoidal signals

The double-frequency term can be neglected because of the narrowband assumption used above. If the estimation error is small, then a linearizing assumption similar to that used in phase-locked loop theory (Ref. 6, p. 18) is that

$$\frac{PC^T}{L} y(t) \approx \frac{P_s}{L} PH^T H(X - \hat{X}) \tag{12}$$

Substitution of this expression into Eq. (10) leads to the baseband linear system shown in Fig. 3. Since the system is linear, one can consider the response of the system to noise separately. Hence, the total input to the linear system is then

$$y(t) = H(t) X(t) + v'(t) \tag{13}$$

where the double-sided spectral density of $v'(t)$ is L/P_s W/Hz. The MMSE estimator (Kalman–Bucy filter) for the observation in Eq. (13) and the stochastic system of Eq. (3) are (Ref. 2, p. 119)

$$\dot{\hat{X}}(t) = \left(A - \frac{P_s}{L} P H^T H\right) \hat{X}(t) + \frac{P_s}{L} P H^T y(t) \tag{14a}$$

$$\hat{X}(0) = E[X(0)] \tag{14b}$$

The NLRE of Eq. (10) becomes the Kalman–Bucy filter of Eq. (14) at high values of SNR.

The error covariance matrix for the above Kalman–Bucy filter is given by the solution to Eq. (11) (Ref. 2, p. 119) which applies to the NLRE of *Subsection* 2. Hence, for large values of the SNR where the linear model is valid, the NLRE becomes a MMSE estimator. For the particular case of rational spectra for $X(t)$, i.e., $A(t)$ is a stability matrix, the steady-state solution of Eq. (11) equals the error covariance of the Wiener optimum linear filter (Ref. 1, p. 42). A steady-state solution of

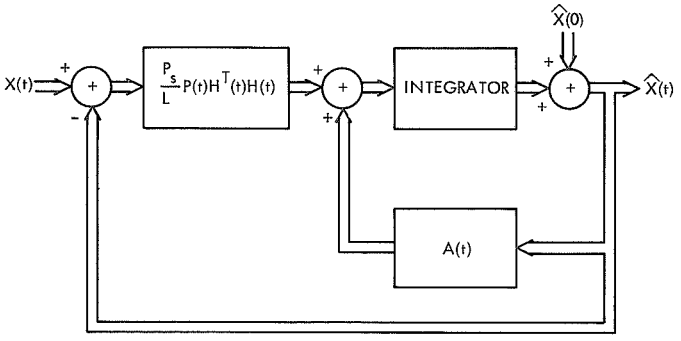

Fig. 3. Equivalent linear baseband estimator

Eq. (11) exists and is unique if A, H, B, and K are continuous functions of time and if A and H form a completely observable system (Ref. 4, p. 62).

The advantage of the state-variable approach is that the specification of the structure and performance of the estimator are easily formulated in matrix notation. The matrix Riccati equation for P in Eq. (11) is especially suited to numerical solution by a digital computer. Generalizations to systems of greater dimensionality require no new conceptual developments. The theory gives exact results for large SNRs and approximate results at low SNRs. Performance evaluation and error bounds in the vicinity of threshold require computer simulation of the algorithm and/or further analytical work.

4. Applications

a. Scalar phase modulation. Consider the stochastic system of Eq. (3) when $A(t) = -a$ and $B(t) = b$ so that $X(t) = x$, a scalar.

$$\dot{x}(t) = -a\,x(t) + b\,u(t) \tag{15}$$

The noise driver $u(t)$ has zero mean with $E[u(t)\,u(t')] = \delta(t - t')$. If $x(t)$ is stationary, then it has a first-order Butterworth spectrum $S_x(\omega)$ with autocorrelation function $R_x(\tau)$, which are given by

$$S_x(\omega) = \frac{b^2}{\omega^2 + a^2}$$

$$R_x(\tau) = \frac{b^2}{2a}\,e^{-a|\tau|}$$

Let the observation be

$$y(t) = g(t) + v(t)$$

or

$$y(t) = (2P_s)^{1/2} \sin[\omega_0 t + x(t)] + v(t) \tag{16}$$

so that the problem is to estimate the phase modulation $x(t)$, assuming that the carrier frequency is known. The noise $v(t)$ has the properties of Eqs. (5b), (5d), and (5e).

Using the narrowband assumption $a << \omega_0$, one obtains the NLRE from Eq. (10),

$$\left.\begin{aligned} \dot{\hat{x}}(t) &= -a\hat{x}(t) + \frac{(2P_s)^{1/2}}{L}\,p(t)\,y(t)\cos[\omega_0 t + \hat{x}(t)] \\ \hat{x}(0) &= 0 \end{aligned}\right\} \tag{17}$$

with $p(t)$ from Eq. (11),

$$\left.\begin{aligned} \dot{p}(t) &= -2ap(t) - \frac{P_s}{L}\,p^2(t) + b^2 \\ p(0) &= \frac{b^2}{2a} \end{aligned}\right\} \tag{18}$$

This system can be implemented as shown in Fig. 4a.

For the scalar case, one can solve Eq. (18) to yield (Ref. 5, p. 64)

$$p(t) = \frac{p(0)}{1 + \dfrac{P_s p(0)}{aL}\,\dfrac{\tanh \gamma a t}{\tanh \gamma a t + \gamma}} \tag{19}$$

where

$$\gamma = \left(\frac{1 + P_s b^2}{a^2 L}\right)^{1/2}$$

For comparison with the Wiener optimum linear filter, the steady-state value $\tilde{p}$ of $p(t)$ is needed. As $t \to \infty$,

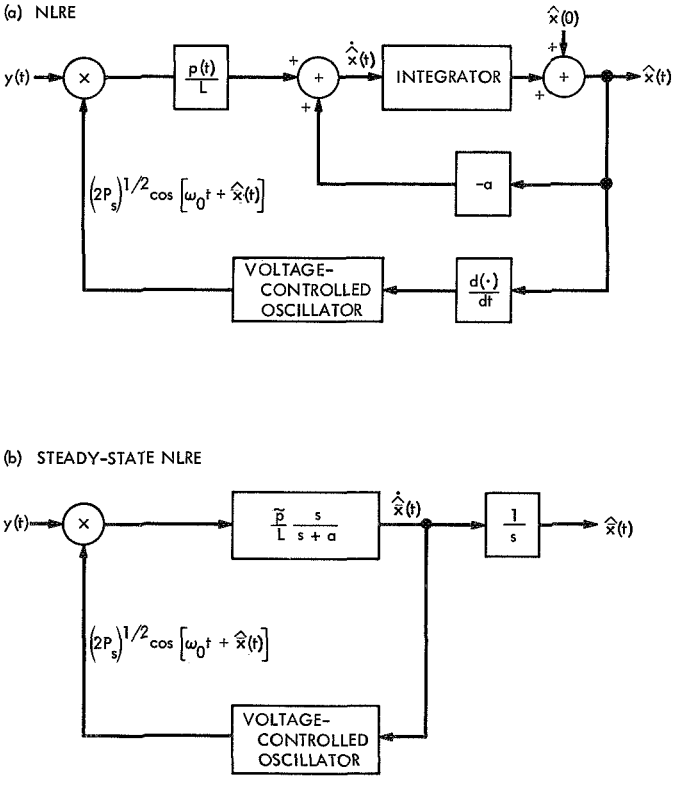

Fig. 4. Systems for scalar phase modulation

Eq. (19) becomes $\tilde{p}$ given by

$$\tilde{p} = \lim_{t\to\infty} p(t) = \frac{aL}{P_s}(\gamma - 1) \tag{20}$$

The steady-state NLRE is given by Eq. (17) with $\tilde{p}$ substituted for $p(t)$. The system can be represented by the block diagram in Fig. 4b, which is a first-order phase-locked loop. This is the Wiener optimum filter in the linear region for tracking phase modulation with no loop detuning (Ref. 6, p. 137). The phase error variance $\sigma^2_{x-\hat{x}}$ can be found by using the Yovits–Jackson formula (Ref. 6, p. 143) and is given by $\tilde{p}$ in Eq. (20).

b. Subcarrier demodulation. An application which demonstrates the extension of the state-variable approach to more complicated systems is given by the addition to the previous example of a subcarrier data channel of known synchronization. Assume the observation to have the form

$$y(t) = (2P_s)^{1/2}\sin[\omega_0 t + x_1(t) + x_2(t)\sin\omega_s t] + v(t) \tag{21}$$

where ω_s is the subcarrier frequency. For simplicity, assume that the statistics of $x_1(t)$ and $x_2(t)$ are given by Eq. (3) with

$$A = \begin{bmatrix} -a_1 & 0 \\ 0 & -a_2 \end{bmatrix}$$

and

$$B = \begin{bmatrix} b_1 & 0 \\ 0 & b_2 \end{bmatrix}$$

The NLRE for this example is given by Eq. (10) with

$$H = [1 \quad \sin\omega_s t] \tag{22}$$

and with the P matrix given by the solution to the set of equations

$$\dot{p}_{11} = -2a_1 p_{11} - \frac{P_s}{L} \times (p_{11}^2 + 2p_{11}p_{21}\sin\omega_s t + p_{21}^2\sin^2\omega_s t) + b_1^2 \tag{23a}$$

$$\dot{p}_{12} = -(a_1 + a_2)p_{12} - \frac{P_s}{L} \times [p_{11}p_{12} + (p_{11}p_{22} + p_{12}^2)\sin\omega_s t + p_{12}p_{22}\sin^2\omega_s t] \tag{23b}$$

$$p_{21} = p_{12} \tag{23c}$$

$$\dot{p}_{22} = -2a_2 p_{22} - \frac{P_s}{L} \times (p_{12}^2 + 2p_{12}p_{22}\sin\omega_s t + p_{22}^2\sin^2\omega_s t) + b_2^2 \tag{23d}$$

In order to gain insight into the operation of the NLRE, assume that the crosscorrelation term p_{12} in Eq. (23) is zero. Then, from Eq. (10) with H given by Eq. (22), one obtains

$$\begin{bmatrix} \dot{\hat{x}}_1 \\ \dot{\hat{x}}_2 \end{bmatrix} = \begin{bmatrix} -a_1\hat{x}_1 \\ -a_2\hat{x}_2 \end{bmatrix} + \frac{(2P_s)^{1/2}}{L}\begin{bmatrix} p_{11} \\ p_{22}\sin\omega_s t \end{bmatrix} y(t)\cos(\omega_0 t + H\hat{X}) \tag{24}$$

The steady-state solution of Eq. (24) can be implemented as shown in Fig. 5.

By neglecting the crosscorrelation between $x_1 - \hat{x}_1$ and $x_2 - \hat{x}_2$, the steady-state NLRE in Fig. 5 is equivalent to

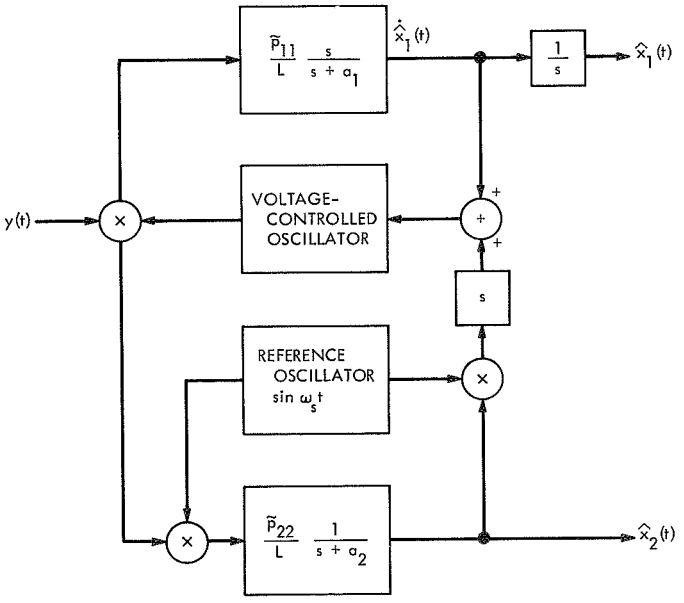

Fig. 5. Steady-state NLRE for subcarrier modulation

the linear MMSE filter obtained by considering x_1 and x_2 as separate modulation processes (Ref. 6, p. 131). The resulting error variances can be found by using the Yovits–Jackson formula (Ref. 6, p. 143) or alternatively by finding the steady-state solution to Eq. (23) with $p_{12} \equiv 0$. Following the latter procedure, one finds the steady-state values $\tilde{p}_{11}$ and $\tilde{p}_{22}$,

$$\tilde{p}_{11} = \frac{\gamma_1 - 1}{2R_1} \tag{25}$$

$$\tilde{p}_{22} = \frac{\gamma_2 - 1}{R_2} \tag{26}$$

where

$$R_i = \frac{P_s}{2La_i}, \qquad i = 1, 2 \tag{27}$$

$$\gamma_1 = [1 + 4R_1 p_{11}(0)]^{1/2} \tag{28}$$

$$\gamma_2 = [1 + 2R_2 p_{22}(0)]^{1/2} \tag{29}$$

where

$$p_{ii}(0) = \frac{b_i^2}{2a_i}, \qquad i = 1, 2 \tag{30}$$

Equations (25) and (26) are plotted in Figs. 6 and 7, respectively; these figures show the variances of each component of phase modulation as a function of the SNR for that component. Following Snyder (Ref. 1, p. 83), a threshold is shown at a level of $\tilde{p}_{ii} = 0.25$ above which the curves give an accurate description of the receiver performance when $p_{12} \equiv 0$.

One would expect that the NLRE would perform better when Eq. (23) is solved without assuming $p_{12} \equiv 0$. However, a numerical solution of this equation has shown that, for this example, $|p_{12}| << p_{11}, p_{22}$ for the range of parameter variations within the narrowband assumption above. Hence, the values of $\tilde{p}_{11}$ and $\tilde{p}_{22}$ given by Eqs. (25) and (26) are applicable in general, and the performance of the NLRE in estimating one state-variable component is essentially independent of the modulation by the other component. For example, the value of $\tilde{p}_{11}$ is invariant with respect to changes of R_2, a_2, or $p_{22}(0)$.

5. Conclusion

The state-variable approach to phase demodulation is particularly suited to the solution of many problems involving a large number of modulation sidebands. In most cases of interest, the method probably does not offer greatly improved performance, but each case should be evaluated against alternative receiver designs. The method does include second-order statistics in the receiver design, and at large values of SNR it does specify the MMSE receiver both for acquisition and steady-state operation. State-variable design techniques can be considered as a means of obtaining realizable system configurations and error variance information. The results presented here provide an evaluation of performance in the linear region of operation, and performance near threshold can be obtained by computer simulation of the

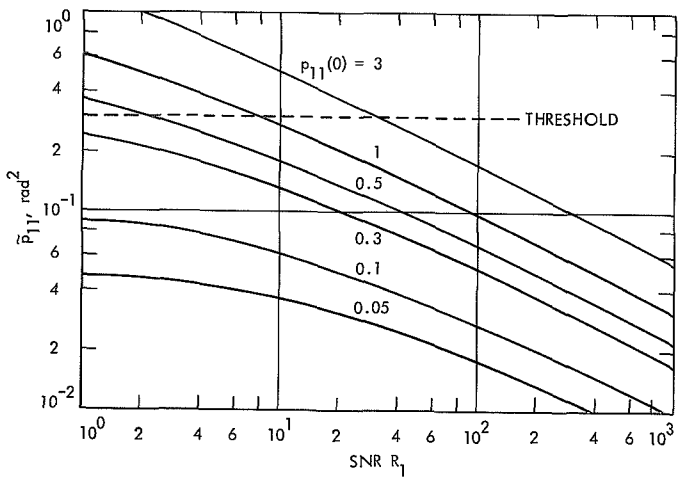

Fig. 6. Variance of $x_1 - \hat{x}_1$ as a function of SNR in bandwidth of $S_{x_1}(\omega)$

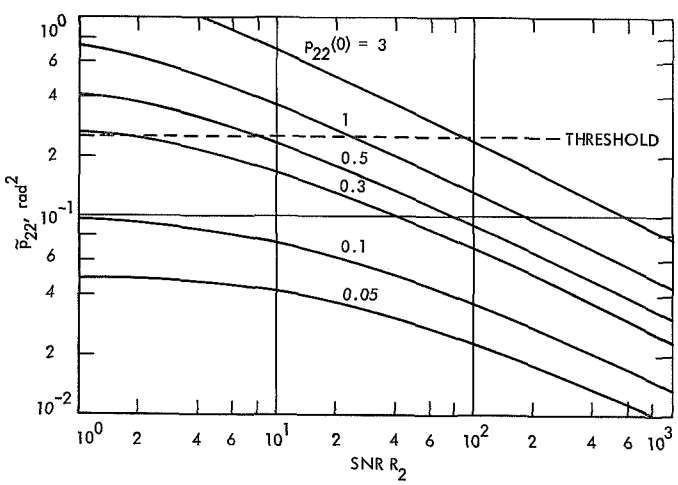

Fig. 7. Variance of $x_2 - \hat{x}_2$ as a function of SNR in bandwidth of $S_{x_2}(\omega)$

NLRE. State-variable analysis gives straightforward results without invoking numerous simplifying assumptions; this advantage becomes more important as the complexity of the system increases.

References

1. Snyder, D. L., *The State-Variable Approach to Continuous Estimation.* The MIT Press, Cambridge, Mass., 1969.

2. Nahi, N. E., *Estimation Theory and Applications.* John Wiley & Sons, Inc., New York, 1969.

3. Schwartz, L., and Stear, E. B., "A Computational Comparison of Several Nonlinear Filters," *IEEE Trans. Auto. Contr.*, Vol. AC-13, No. 1, pp. 83–86, Feb. 1968.

4. Bucy, R. S., and Joseph, P. D., *Filtering for Stochastic Processes with Applications to Guidance.* Interscience Publishers, Inc., New York, 1968.

5. Brand, L., *Differential and Difference Equations.* John Wiley & Sons, Inc., New York, 1966.

6. Viterbi, A. J., *Principles of Coherent Communication.* McGraw-Hill Book Co., Inc., New York, 1966.